

Charm Tetraquark Production by Intrinsic Charm

R. Vogt

Lawrence Livermore National Laboratory, Livermore, CA 94551, USA
Physics and Astronomy Department, UC Davis, Davis, CA 95616, USA



U.S. DEPARTMENT OF
ENERGY

Office of
Science



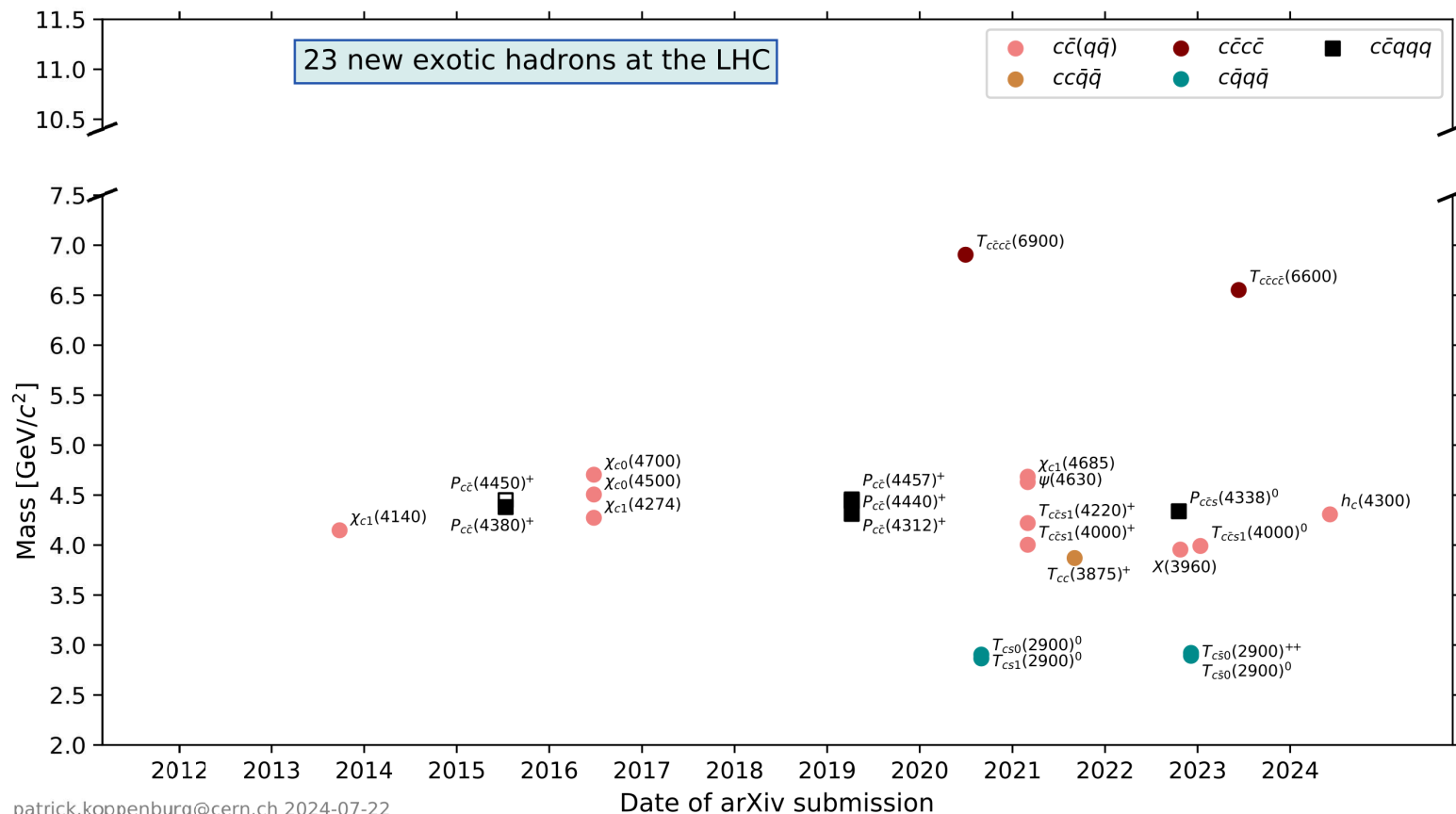
Figure 1: This work was performed under the auspices of the U.S. Department of Energy by Lawrence Livermore National Laboratory under Contract DE-AC52-07NA27344, the LLNL-LDRD Program under Projects 21-LW-034 and 23-LW-036 and the HEFTY Collaboration.

What are Tetraquarks?

Standard mesons and baryons are composed of $q\bar{q}$ and qqq respectively

No need to stop at those, Murray Gell-Mann, when coming up with “quarks”, also noted that states like $q\bar{q}q\bar{q}$ (tetraquarks), $qqqq\bar{q}$ (pentaquarks), and more could exist.

The $X(3872)$ was the first such state to be discovered, at Belle in 2003; lately many new “exotic” states have been found at the LHC, see below for exotic state production as a function of time

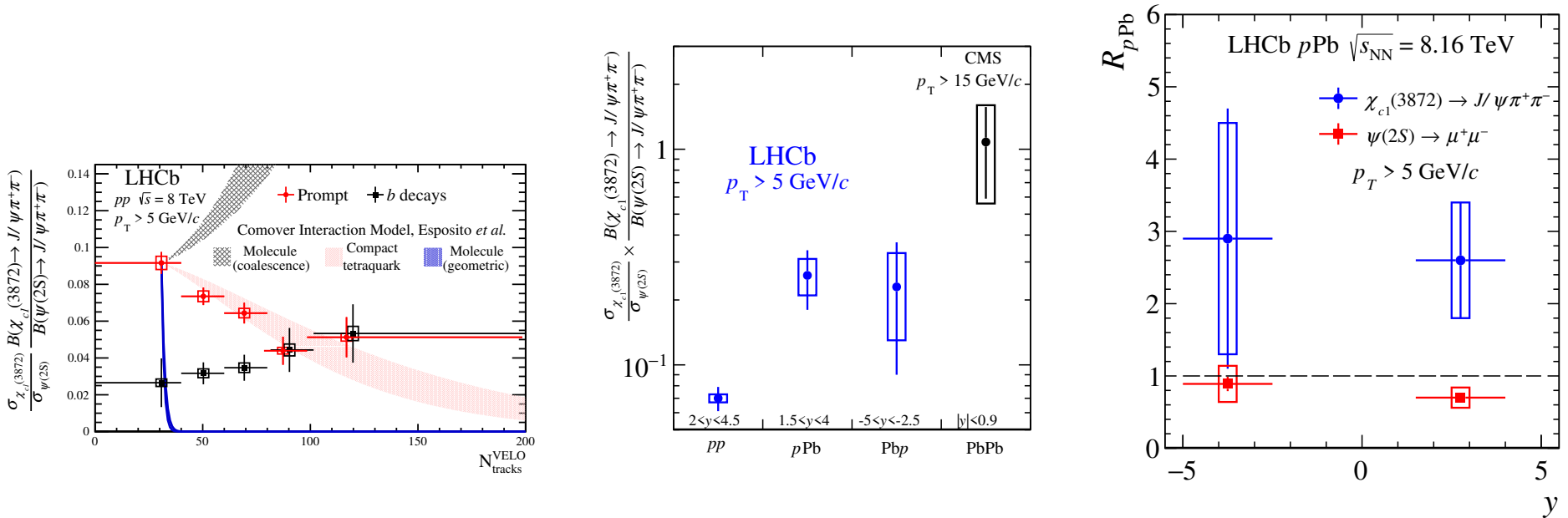


The $X(3872)$ Has Been Measured In Medium

(Left) The ratio $X(3872)/\psi(2S)$ decreases with multiplicity in $p+p$ collisions at 8 TeV (LHCb, Phys. Rev. Lett. 126, 092001 (2021))

(Center) The multiplicity-integrated ratio $X(3872)/\psi(2S)$ increases from $p+p$ to $p+Pb$ to $Pb+Pb$ collisions (LHCb, Phys. Rev. Lett. 132, 242301 (2021), $Pb+Pb$ results from CMS in Phys. Rev. Lett 128, 032001 (2022)). Note that the LHCb results are at forward (and backward in $Pb+p$) while the CMS results are at midrapidity. Also, the CMS results are over higher p_T .

(Right) To determine which of the two, $X(3872)$ or $\psi(2S)$, produces the enhancement seen, LHCb determined R_{pPb} of each one separately – the $X(3872)$ is clearly enhanced, albeit with large uncertainties.



Tetraquark Production by Intrinsic Charm

While $X(3872)$ is the best measured of the tetraquark candidates, there are many others that could also be studied in medium

Their production was studied in $p+p$ collisions by intrinsic charm in arXiv:2405.09018

| State | Mass (MeV) | Quark Content | Reference |
|------------------------------|--------------------------------|--------------------------|--|
| states with 4 charm quarks | | | |
| $T_{\psi\psi}(6600)$ | 6630 ± 90 6552 ± 16 | $\bar{c}\bar{c}c\bar{c}$ | ATLAS, Phys. Rev. Lett. 131 , 151902 (2023) CMS, arXiv:2306.07164 [hep-ex] |
| $T_{\psi\psi}(6900)$ | 6905 ± 13 | $\bar{c}\bar{c}c\bar{c}$ | LHCb, Sci. Bull. 65 , 1983-1993 (2020) |
| states with 2 charm quarks | | | |
| $X(3872)$ | 3872 ± 0.6 | $c\bar{u}c\bar{u}$ | Belle, Phys. Rev. Lett. 91 , 262001 (2003) |
| $X_s(3960)$ | 3955 ± 13 | $\bar{c}\bar{s}c\bar{s}$ | LHCb, Phys. Rev. Lett. 131 , 071901 (2023) |
| $X_s(4274)$ | 4273_{-9}^{+10} | | LHCb, Phys. Rev. Lett. 118 , 022003 (2017) |
| $X_s(4500)$ | 4506_{-19}^{+16} | | LHCb, Phys. Rev. Lett. 118 , 022003 (2017) |
| $X_s(4630)$ | 4630_{-110}^{+20} | | LHCb, Phys. Rev. Lett. 127 , 082001 (2021) |
| $X_s(4685)$ | 4684_{-17}^{+15} | | LHCb, Phys. Rev. Lett. 127 , 082001 (2021) |
| $X_s(4700)$ | 4704_{-26}^{+17} | | LHCb, Phys. Rev. Lett. 118 , 022003 (2017) |
| $T_{cc}^+(3876)$ | 3870 ± 0.12 | $c\bar{c}u\bar{d}$ | LHCb, Nature Phys. 18 , 751-754 (2022) |
| $T_{c\bar{c}s1}^0(4000)$ | 3991_{-20}^{+14} | $\bar{c}\bar{c}d\bar{s}$ | LHCb, Phys. Rev. Lett. 131 , 131901 (2023) |
| $T_{c\bar{c}s1}^+(4220)$ | 4220_{-40}^{+50} | $\bar{c}\bar{c}u\bar{s}$ | LHCb, Phys. Rev. Lett. 127 , 082001 (2021) |
| states with 1 charm quark | | | |
| $T_{c\bar{s}0}^a(2900)^0$ | 2892 ± 21 | $\bar{c}\bar{s}u\bar{d}$ | LHCb, Phys. Rev. Lett. 131 , 041902 (2023) |
| $T_{c\bar{s}0}^a(2900)^{++}$ | 2921 ± 25 | $\bar{c}\bar{s}u\bar{d}$ | LHCb, Phys. Rev. Lett. 131 , 041902 (2023) |
| $T_{cs0}(2900)^0$ | 2866 ± 7 | $cds\bar{u}$ | LHCb, Phys. Rev. D 102 , 112003 (2020) |
| $T_{cs1}(2900)^0$ | 2904 ± 5 | | LHCb, Phys. Rev. D 102 , 112003 (2020) |

Table 1: Some of the new particles designated as tetraquark candidates, along with their mass and assigned quark content. Note that the X_s states, as denoted here, are often only referred to as X states. A distinction is made here for the strange quark content. See also <https://qwg.ph.nat.tum.de/exoticshub/> and <https://www.nikhef.nl/pkoppenn/particles.html>.

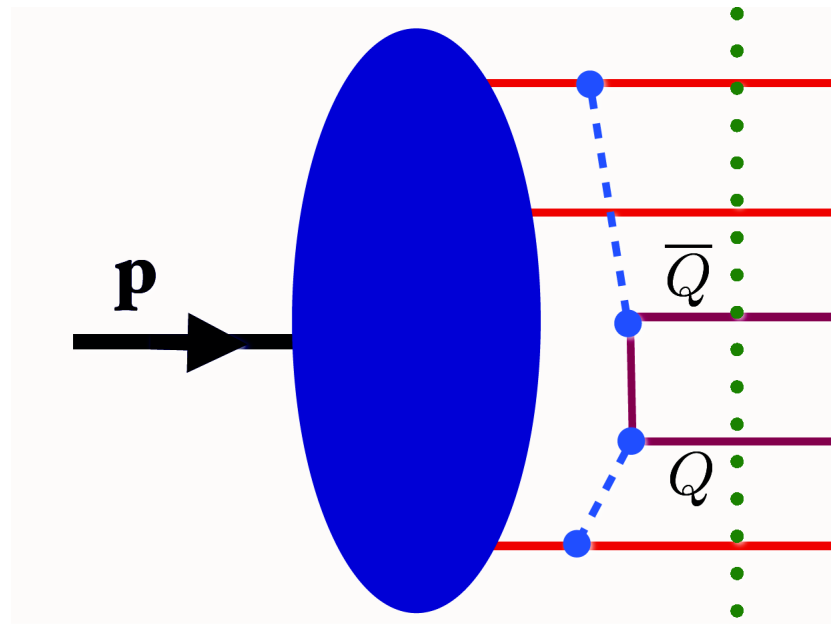
What is Intrinsic Charm?

Proton wavefunction can be expanded as sum over complete basis of quark and gluon states: $|\Psi_p\rangle = \sum_m |m\rangle \psi_{m/p}(x_i, k_{T,i}, \lambda_i)$

$|m\rangle$ are color singlet state fluctuations into Fock components $|uud\rangle, |uudg\rangle \cdots |uudc\bar{c}\rangle$

The intrinsic charm fluctuations can be freed by a soft interaction if the system is probed during the time $\Delta t = 2p_{\text{lab}}/M_{c\bar{c}}^2$ that the fluctuations exist

Dominant Fock state configurations have minimal invariant mass, $M^2 = \sum_i m_{T,i}^2/x_i$, where $m_{T,i}^2 = k_{T,i}^2 + m_i^2$ is the squared transverse mass of parton i in the state; corresponds to configurations with equal rapidity constituents



Intrinsic Charm is a Long-Standing Puzzle in QCD

Intrinsic charm in the proton $|uudc\bar{c}\rangle$, was first proposed in the 1980's

If this state dominates the wavefunction, the charm quarks carry a larger fraction of the hadron momentum, enhancing charm production in the forward x_F region

A number of experimental hints have been seen, no conclusive results

- Charm structure function, F_2^c , large at largest x and highest Q^2 measured (EMC)
- Leading charm asymmetries consistent with intrinsic charm predictions (D^- over D^+ in π^-p interactions, E791)
- Double J/ψ production observed at high pair x_F by NA3
- Forward charm production observed in many fixed-target experiments (WA82, WA89, E791, SELEX and others)
- Proposed explanation of high energy astrophysical neutrino rate at Ice Cube (Brodsky and Laha)
- LHCb $Z+c$ -jet measurements at forward rapidity consistent with intrinsic charm

Global PDF analyses have tried incorporating intrinsic charm and reported a range of possible contributions from 0 to 1%, most lately the NNPDF Collaboration (Nature) and the CTEQ Collaboration

At colliders, intrinsic charm is boosted to high rapidity and detection is less likely, fixed-target configurations may be better for discovery measurement

Heavy Flavor Production by Intrinsic Charm

Probability distribution of five-particle Fock state of the proton:

$$dP_{\text{ic}5} = P_{\text{ic}5}^0 N_5 \int dx_1 \cdots dx_5 \int dk_{x1} \cdots dk_{x5} \int dk_{y1} \cdots dk_{y5} \frac{\delta(1 - \sum_{i=1}^5 x_i) \delta(\sum_{i=1}^5 k_{xi}) \delta(\sum_{i=1}^5 k_{yi})}{(m_p^2 - \sum_{i=1}^5 (\hat{m}_i^2/x_i))^2}$$

$i = 1, 2, 3$ are u, u, d light quarks, 4 and 5 are c and \bar{c} , N_t normalizes the probability to unity and P_{ic}^0 scales the normalized probability to the assumed intrinsic charm content: 0.1%, 0.31% and 1% are used to represent the range of probabilities assumed previously (based on original Brodsky *et al.* model)

The IC cross section is determined from soft interaction scale breaking coherence of the Fock state, $\mu^2 = 0.1 \text{ GeV}^2$

$$\sigma_{\text{ic}}(pp) = P_{\text{ic}5} \sigma_{pN}^{\text{in}} \frac{\mu^2}{4\hat{m}_c^2}$$

The cross sections from intrinsic charm are then obtained by multiplying by the normalization factor for the CEM to the J/ψ while we assume direct correspondence with IC cross section for \bar{D}^0

$$\sigma_{\text{ic}}^{\bar{D}^0}(pp) = \sigma_{\text{ic}}(pp) \quad , \quad \sigma_{\text{ic}}^{J/\psi}(pp) = F_C \sigma_{\text{ic}}(pp)$$

Other assumptions of intrinsic charm distributions in the nucleon are the meson cloud model ($c(x) \neq \bar{c}(x)$) and a sea-like distribution ($c(x) = \bar{c}(x) \propto \bar{d}(x) + \bar{u}(x)$)

Tetraquark Masses can be Calculated by Intrinsic Charm

Tetraquark production by intrinsic charm states can be studied by extending intrinsic charm from 5-particle states to 7- and 9-particle Fock states

States with more than 9 particles are not considered, if a tetraquark candidate state requires more than that, the antiparticle is studied: the $T_{cc}^+(cc\bar{u}\bar{d})$ requires an 11-particle state, $|uudc\bar{c}\bar{c}u\bar{u}\bar{d}\bar{d}\rangle$, so so the $T_{cc}^-(\bar{c}\bar{c}ud)$ (7-particle state), is studied

The k_T integration range represents the range of motion of quarks in the system, smaller ranges would indicate tighter binding and lower mass while larger ranges suggest more loosely bound, higher mass systems, similar to a difference between ground and excited states

Some of the candidate states can be considered to be bound meson pairs while others can only be bound (produce a mass peak) if the constituent partons are uncorrelated (independent of each other)

Tetraquarks consisting of tightly bound meson pairs may be broken up into two individual mesons and (re)-produced by coalescence of pairs of D mesons in high multiplicity environments while those made of uncorrelated partons (with wider widths) may break up more easily initially with production by coalescence also possible

Interactions of tetraquarks with medium will depend on their internal structure

Tetraquarks as Meson Pairs

Start from basic “ n ” particle probability distribution

$$dP_{\text{ic}n} = P_{\text{ic}n}^0 N_n \int dx_1 \cdots dx_n \int dk_{x1} \cdots dk_{xn} \int dk_{y1} \cdots dk_{yn} \frac{\delta(1 - \sum_{i=1}^n x_i) \delta(\sum_{i=1}^n k_{xi}) \delta(\sum_{i=1}^n k_{yi})}{(m_p^2 - \sum_{i=1}^n (m_{Ti}^2/x_i))^2}$$

Then constrain the kinematics of the meson pair

This results in a fairly narrow mass distribution for low internal k_T of the constituent partons

$$\begin{aligned} \frac{dP_{\text{ic}n}}{dM_{\text{TQ}}^2} &= \int \frac{dx_{M_1}}{x_{M_1}} \frac{dx_{M_2}}{x_{M_2}} \int dm_{M_1}^2 dm_{M_2}^2 \int dk_{xM_1} dk_{yM_1} dk_{xM_2} dk_{yM_2} \int \frac{dx_{\text{TQ}}}{x_{\text{TQ}}} \int dk_{x\text{TQ}} dk_{y\text{TQ}} dP_{\text{ic}n} \\ &\times \delta\left(\frac{m_{T,M_1}^2}{x_{M_1}} - \frac{m_{T4}^2}{x_4} - \frac{m_{T7}^2}{x_7}\right) \delta(k_{x4} + k_{x7} - k_{xM_1}) \delta(k_{y4} + k_{y7} - k_{yM_1}) \delta(x_{M_1} - x_4 - x_7) \\ &\times \delta\left(\frac{m_{T,M_2}^2}{x_{M_2}} - \frac{m_{T5}^2}{x_5} - \frac{m_{T6}^2}{x_6}\right) \delta(k_{x5} + k_{x6} - k_{xM_2}) \delta(k_{y5} + k_{y6} - k_{yM_2}) \delta(x_{M_2} - x_5 - x_6) \\ &\times \delta\left(\frac{M_{T,\text{TQ}}^2}{x_{\text{TQ}}} - \frac{m_{T,M_1}^2}{x_{M_1}} - \frac{m_{T,M_2}^2}{x_{M_2}}\right) \delta(k_{xM_1} + k_{xM_2} - k_{x\text{TQ}}) \delta(k_{yM_1} + k_{yM_2} - k_{y\text{TQ}}) \delta(x_{\text{TQ}} - x_{M_1} - x_{M_2}) \end{aligned}$$

Tetraquarks as Four Independent Partons

In some cases, such as $T_{\psi_s}(c\bar{c}s\bar{u})$, treating the state as a meson pair means that the “light” meson orbits around a more stationary heavy one and assuming a higher mass of the tetraquark means that the light meson gets further away and less bound

Release the kinematic constraints for meson pairs and conserve momentum among individual partons

These mass distributions are broader than the meson pair assumption and thus potentially less bound

$$\begin{aligned} \frac{dP_{icn}}{dM_{TQ}^2} &= \int \frac{dx_{TQ}}{x_{TQ}} \int dk_{xTQ} dk_{yTQ} dP_{icn} \delta \left(\frac{M_{T,TQ}^2}{x_{TQ}} - \frac{m_{T,4}^2}{x_4} - \frac{m_{T,5}^2}{x_5} - \frac{m_{T,6}^2}{x_6} - \frac{m_{T,7}^2}{x_7} \right) \\ &\times \delta(k_{x4} + k_{x5} + k_{x6} + k_{x7} - k_{xTQ}) \delta(k_{y4} + k_{y5} + k_{y6} + k_{y7} - k_{yTQ}) \\ &\times \delta(x_{TQ} - x_4 - x_5 - x_6 - x_7) \end{aligned}$$

Tetraquark Mass Distributions from Intrinsic Charm

(Left) $X(3872)$ as a $D\bar{D}$ meson pair

(Right) $T_{c\bar{c}s}$ as four independent partons

“ktX” indicates the k_T integration range with kt2 the smallest and kt3 the largest

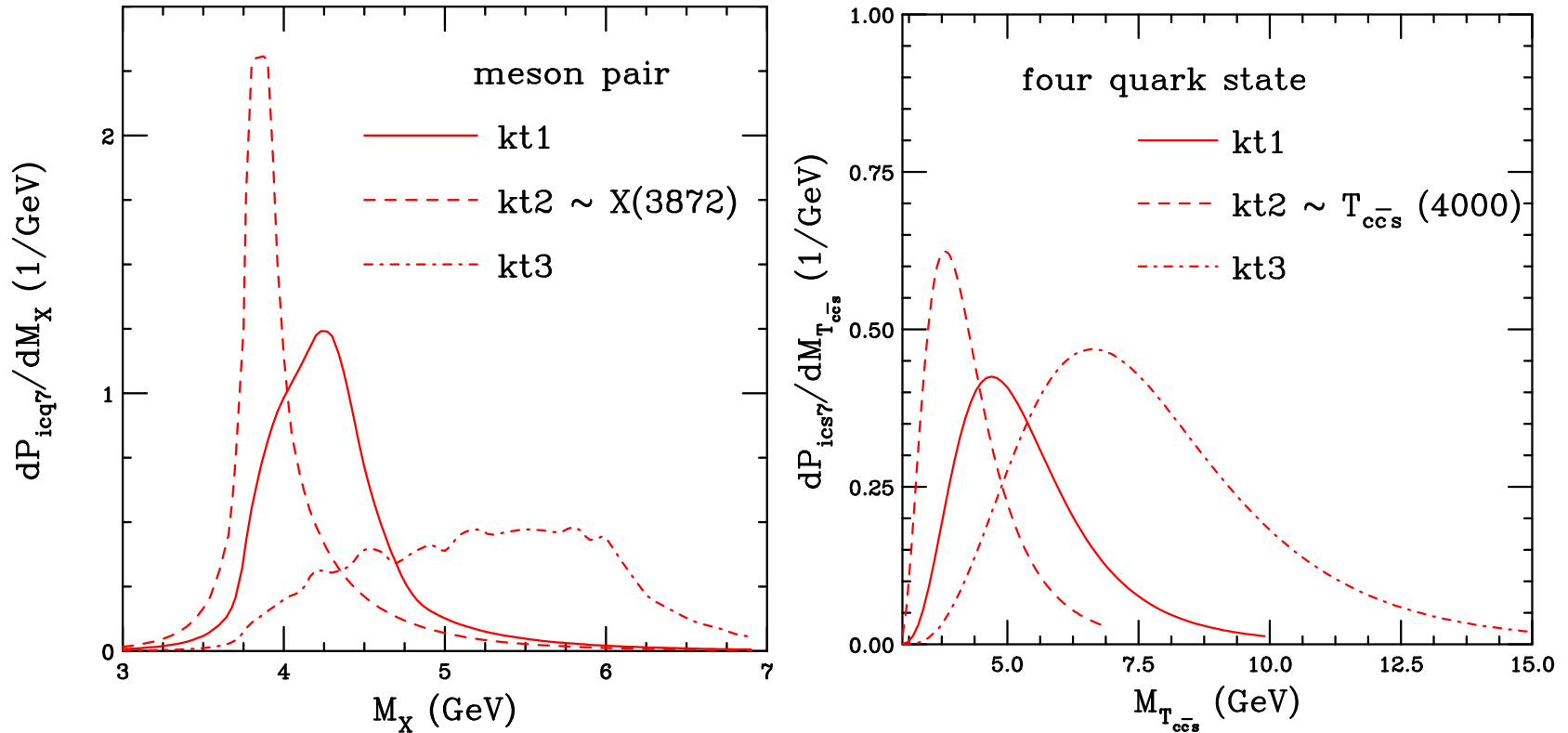


Figure 3: (Left) The $X(3872)$ probability distribution, calculated assuming that the X is a bound meson pair as a function of mass of the state. (Right) The $T_{c\bar{c}s}$ probability distribution, calculated assuming as a function of mass of the state. Calculations are made for different assumptions of the k_T integration range. (RV, arXiv:2405.09018.)

Tetraquark Kinematic Distributions at the LHC

The $X(3872)$ is boosted to high rapidity at the LHC (left)

High rapidity corresponds to low p_T in the calculation to satisfy the minimization of the intrinsic charm probability, making rapidity cuts below the peak of the distribution remove the low p_T part of the spectrum (right)

The range of the LHCb acceptance captures only about 0.1% of the intrinsic charm distribution at 13 TeV, a bit more at 5 TeV

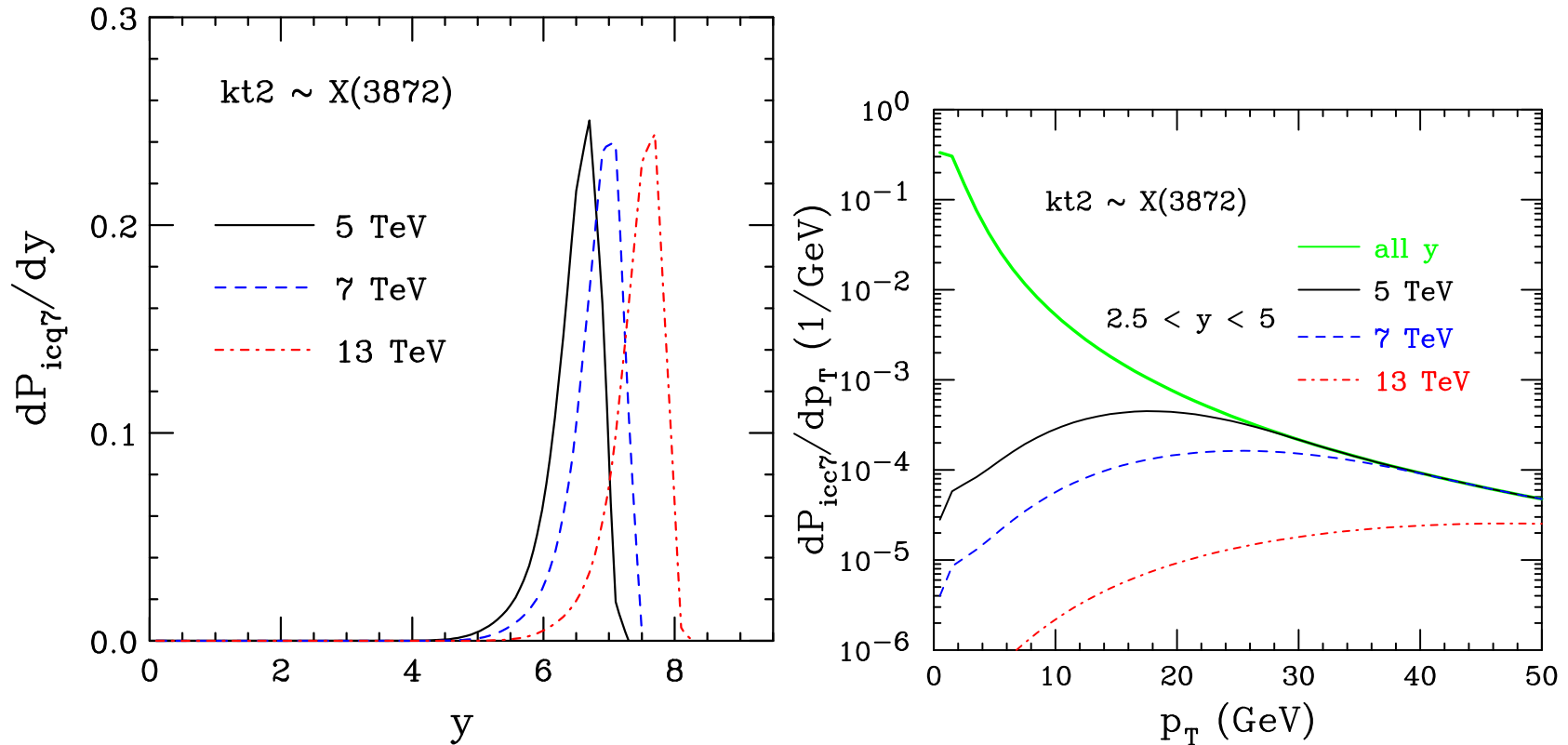


Figure 4: (Left) The probability distribution as a function of rapidity (left) and p_T (right) for $X(3872)$ production at $\sqrt{s} = 5$ (solid black), 7 (dashed blue), and 13 TeV (dot-dashed red), all calculated using parameter set kt2. (RV, arXiv:2405.09018.)

Can Intrinsic Charm Affect Production at the LHC?

(Left) The improved color evaporation model can describe the LHCb data at 13 TeV very well without intrinsic charm (IC on the plot)

(Right) At 5 TeV and high p_T the ICEM and intrinsic charm contributions become comparable

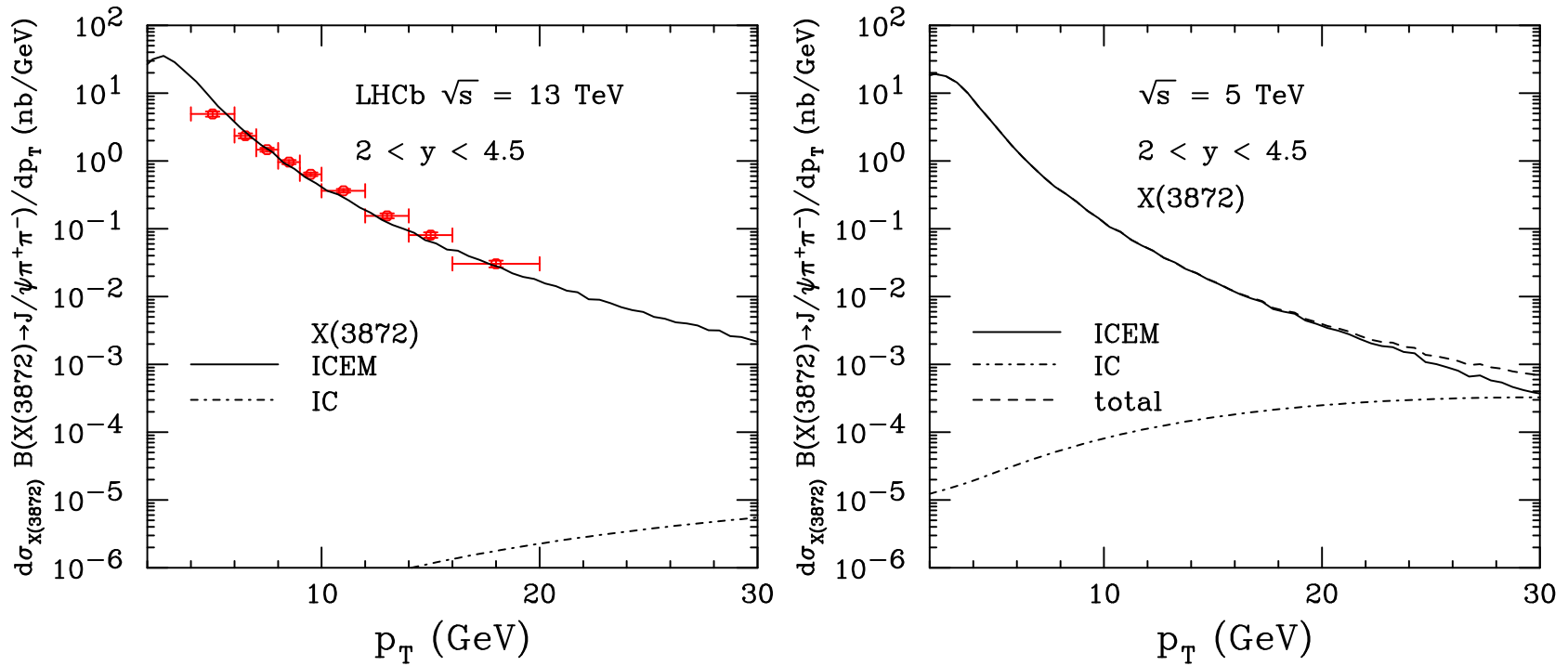


Figure 5: (Left) The $X(3872)$ p_T distribution from the ICEM (solid) and intrinsic charm (dot-dashed) contributions at $\sqrt{s} = 13$ TeV in the rapidity interval $2 < y < 4.5$. The same calculation at 5 TeV. (RV, arXiv:2405.09018.)

Production of Other Tetraquark States Is Similar

The small intrinsic charm contribution at high p_T at 13 TeV is not surprising based on the rapidity distributions (left), the rapidity range of the LHCb data captures only about 0.1% of the intrinsic charm distribution at 13 TeV

The lower energy of 5 TeV captures more of the p_T distribution, making the contribution competitive with the perturbative one at high p_T

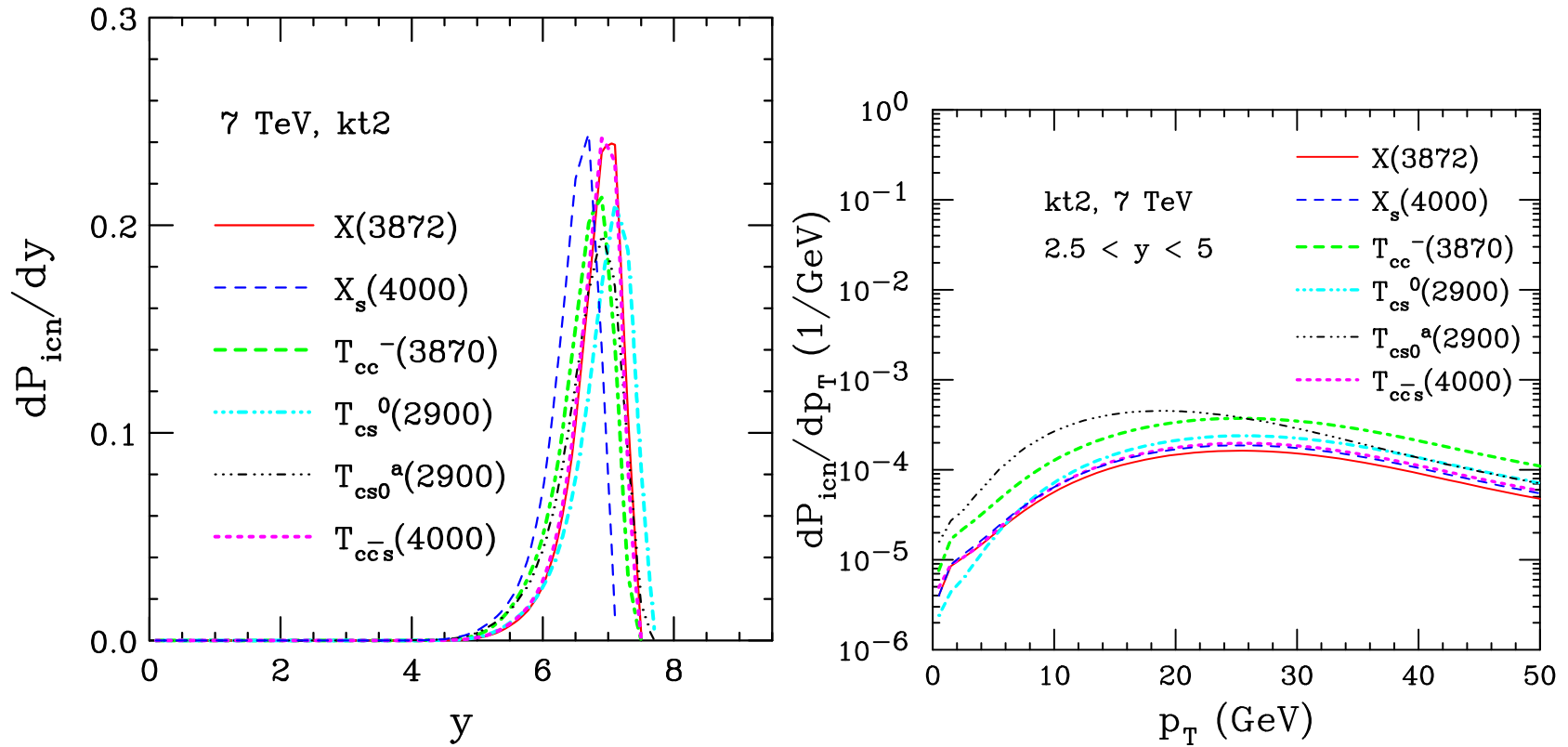


Figure 6: The probability distribution as a function of rapidity (left) and p_T (right) at $\sqrt{s} = 7$ TeV using parameter set kt2 for $X(3872)$ (solid red), X_s (dashed blue), T_{cc}^- (dot-dashed green); T_{cs0}^a (dot-dot-dot-dashed black), T_{cs}^0 (dash-dash-dash-dotted cyan) and T_{ccs}^- (dotted magenta). (RV, arXiv:2405.09018.)

$X(3872)$ Production at the EIC

Assume that the tetraquark candidate is produced in the proton along its direction. Looked at rapidity and p_T distributions for $E_p = 41, 100$ and 275 GeV; p_T distributions are calculated for $0 < y < 2$ and $2 < y < 4$.

At central rapidities, the tetraquark can take up a large fraction of the energy. Note that high p_T corresponds to $y \rightarrow 0$ while low p_T for intrinsic charm corresponds to high rapidity. The higher the proton energy, the more the tetraquark moves to higher rapidity and the less of its distribution is captured in the central region. On the other hand, at low E_0 there is no phase space for production at forward rapidity and high p_T , only the highest proton beam energy captures most of the rapidity distribution.

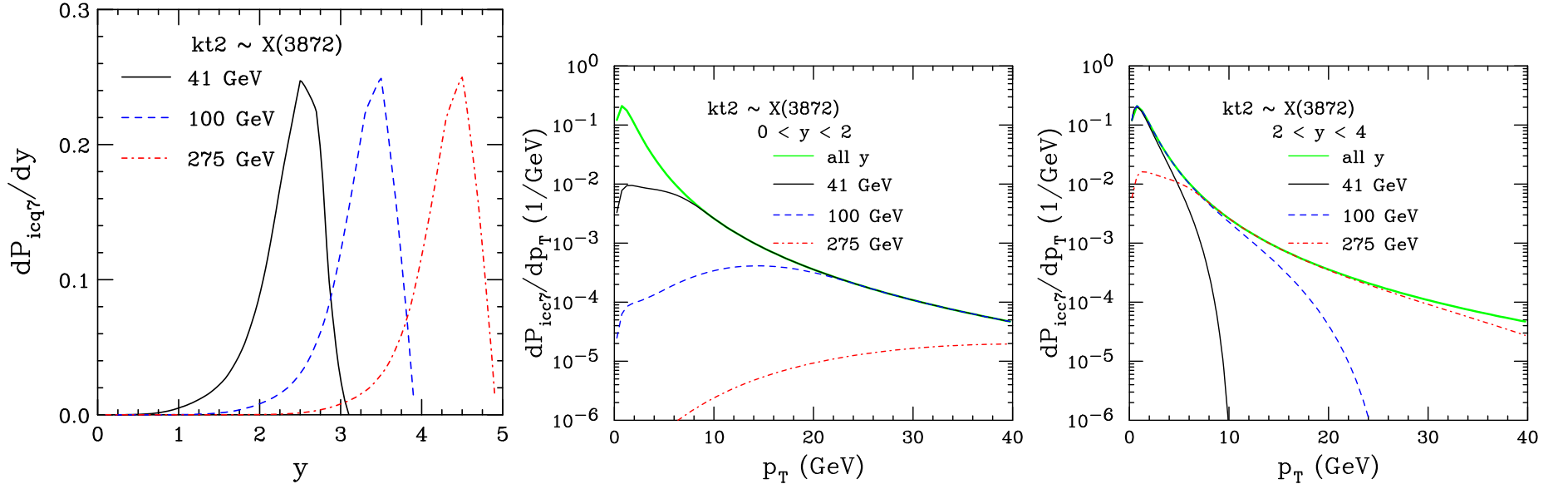


Figure 7: (Left) The $X(3872)$ y distribution from intrinsic charm for $E_p = 41, 100,$ and 275 GeV. The p_T distributions at the same energies are shown for $0 < y < 2$ (Center) and $2 < y < 4$ (Right).

Summary

A variety of heavy tetraquark candidates have been measured at the LHC

The $X(3872)$ tetraquark has already been measured in medium by LHCb ($p + \text{Pb}$) and CMS (Pb+Pb)

Tetraquarks can be produced at forward rapidity by intrinsic charm

Intrinsic charm-like states could be used to study exotic hadron production, can distinguish between types of internal tetraquark structure

Lower energies would put the bulk of tetraquarks production by this mechanism closer to midrapidity, enhancing the possibility of seeing contributions to production by this mechanism

Tetraquark production should be studied with SMOG at LHCb and at the EIC

Thank You!